Molecular Cell, Vol. 2, 437–445, October, 1998, Copyright ©1998 by Cell Press

Localization of *ASH1* mRNA Particles in Living Yeast

Edouard Bertrand,[†] Pascal Chartrand, Matthias Schaefer,[‡] Shailesh M. Shenoy, Robert H. Singer,* and Roy M. Long[§]
Department of Anatomy and Structural Biology and Cell Biology
Albert Einstein College of Medicine
Bronx, New York 10461

Summary

***ASH1* mRNA localizes to the bud tip in *Saccharomyces cerevisiae* to establish asymmetry of HO expression, important for mating type switching. To visualize real time localization of the mRNA in living yeast cells, green fluorescent protein (GFP) was fused to the RNA-binding protein MS2 to follow a reporter mRNA containing MS2-binding sites. Formation and localization of a GFP particle in the bud required *ASH1* 3′UTR (untranslated region) sequences. The *SHE* mutants disrupt RNA and particle localization and *SHE* 2 and 3 mutants inhibit particle formation as well. Both She3myc and She1myc colocalized with the particle. Video microscopy demonstrated that She1p/Myo4p moved particles to the bud tip at 200–440 nm/sec. Therefore, the *ASH1* 3′UTR-dependent particle serves as a marker for RNA transport and localization.**

Introduction

Messenger RNA localization is a well documented phenomenon and provides a mechanism by which to generate cell asymmetry (St. Johnston, 1995; Glotzer and Ephrussi, 1996; Steward and Singer, 1997). For instance, regulation of mating type switching in yeast (Strathern and Herskowitz, 1979) requires the asymmetric concentration of a determinant, Ash1p, within the daughter nucleus relative to the mother nucleus (Bobola et al., 1996; Sil and Herskowitz, 1996). This asymmetric targeting postanaphase of Ash1p represses transcription of the HO endonuclease in the daughter cell, to prevent switching (reviewed by Amon, 1996). We have demonstrated that this asymmetric distribution of Ash1p to daughter nuclei requires localization of its mRNA at the bud tip (Long et al., 1997; Takizawa et al., 1997). The protein can therefore be locally synthesized and transported into the daughter nucleus. The mechanism by which *ASH1* mRNA moves to the bud tip is unknown. However, two aspects are known: one is that sequences in the 3′UTR of *ASH1* mRNA are sufficient for localization and that all of the five *SHE* genes that are required for the asymmetric repression of mating type switching affect mRNA localization. One of these genes is *SHE1/MYO4*, a type V myosin specific for the localization of the mRNA (Long et al., 1997; Takizawa et al., 1997). Myo4p also is localized to the bud tip during anaphase. An intact actin cytoskeleton is also required for localization of the mRNA. We have hypothesized that either the myosin is directly involved in RNA transport on actin cables, or it is indirectly involved by transporting an anchor that subsequently binds the RNA to the bud cortex (Long et al., 1997). Distinguishing between these mechanisms requires a method to characterize RNA movement within the sub-second time frame of a motor molecule.

The current method to visualize RNA in yeast by fluorescent in situ hybridization (FISH) (Long et al., 1995) is not adequate to answer questions of RNA movement because it lacks the temporal resolution obtainable from living cells. For instance, if a motor were involved in moving the RNA, the speeds, ranging as high as .5 μ per second, would be much faster than could be approached by any genetic or synchronized cell procedure that requires fixation of the cells. Clearly, a method was necessary wherein the RNA in a cell can be observed through a rapid series of observations. We therefore developed the means to monitor RNA movement in living yeast cells. The time resolution afforded by this approach strongly suggested that the mRNA was moved by a myosin motor and showed that the process of localization took only a few minutes.

Such a method will have general utility in the RNA transport field, as well as addressing immediate questions concerning the mechanism of *ASH1* mRNA localization.

Results

A Method To Follow mRNA in Living Cells

Currently, no method exists to visualize native RNA in living cells. A novel approach was therefore developed to visualize RNA movement in real time in living cells. We constructed a two-plasmid system in yeast. On one plasmid, the GFP sequence was fused to coding sequences for the single-stranded RNA phage capsid protein MS2 (Fouts et al., 1997). On the second plasmid, six MS2-binding sites, each consisting of a 19-nucleotide RNA stem loop (Valegard et al., 1997) were inserted into a reporter mRNA (Figure 1A), to provide increased signal from multiple bound GFPs. A nuclear-localization signal was engineered into this GFP-MS2 chimera so that it would be restricted to the nucleus if not complexed to RNA. The GFP-MS2 fusion protein was expressed from the strong constitutive *GPD* promoter (Schena et al., 1991), while the reporter mRNA was under control of a galactose-inducible promoter (Long et al., 1995).

* To whom correspondence should be addressed (e-mail: rhsinger@aecom.yu.edu).
[†] Present address: Institut de Genetique Moleculaire de Montpellier, CNRS, 1919 route de Mende, BP 5051, 34033 Montpellier Cedex 01, France.
[‡] Present address: Research Institute of Molecular Pathology, A-1030 Vienna, Austria.
[§] Present address: Department of Microbiology and Molecular Genetics, Medical College of Wisconsin, 8701 Watertown Plank Road, Milwaukee, Wisconsin 53226-0509.

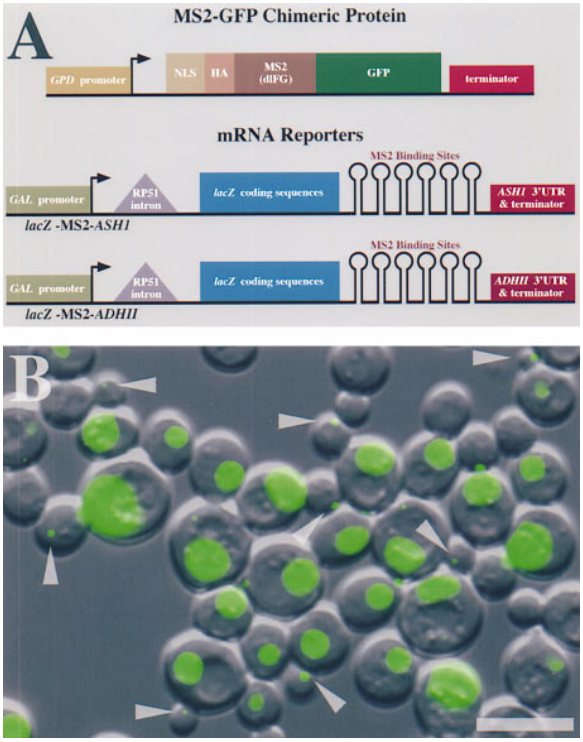

Figure 1. Visualization of Reporter mRNAs in Live Cells

(A) Schematic describing the constructs used in this approach. The system is comprised of two components, a reporter mRNA and a GFP-MS2 fusion protein. The GFP-MS2 was expressed under the control of the constitutive *GPD* promoter, while the reporter mRNA was under the control of the *GAL* promoter. The reporter mRNA contains six binding sites for the coat protein of the bacterial phage MS2. To avoid possible interference with translation and the function of the 3′UTR, the MS2-binding sites were introduced immediately after a translation termination codon. The 3′UTRs were either from the *ASH1* gene, to induce mRNA localization at the bud tip, or from the *ADHII* gene, as control. In addition, a nuclear localization signal (NLS) followed by an HA tag was introduced at the N terminus of the fusion protein, so that that only the GFP protein that is bound to its target mRNA would be present in the cytoplasm.

(B) Live cells expressing the GFP-MS2 fusion protein and the *lacZ*-MS2-*ASH1* reporter mRNA. Arrows indicate some of the particles, usually in the bud. Bar, 5 μm.

The *ASH1* 3′UTR Induces the Formation of Particles

As a reporter for RNA localization, we used the *ASH1* mRNA 3′UTR fused to a *lacZ* construct (the *lacZ*-MS2-*ASH1* mRNA referred to as the *ASH1* reporter) that we previously used to identify a *cis*-acting element sufficient for localization of a reporter RNA to buds, as demonstrated by FISH (Long et al., 1997). Yeast cells expressing both the GFP-MS2 chimera and the *ASH1* reporter contained a single, bright particle that was usually localized at the bud tip (referred to as the "particle"; Figures 1B and 2A, right). To determine whether particle formation and its localization were dependent on the *ASH1* 3′UTR, we substituted the *ADHII* 3′UTR in place of the *ASH1* 3′UTR. This sequence was unable to localize a reporter RNA to the bud tip (Long et al., 1997). The GFP-MS2 chimera expressed with this construct was diffuse in its distribution throughout the cytoplasm (Figure 2B, right). This result is consistent with the observation that the *lacZ-ADHII* mRNA reporter does not localize (Long et al., 1997).

To show that the bright particles originated from GFP-MS2 bound to the *ASH1* reporter, we performed FISH with probes specific for *lacZ* (or MS2; data not shown). In cells expressing the *ASH1* reporter, its mRNA colocalized with the GFP-MS2 in the particle (Figure 2A). Likewise, when the *ADHII* reporter was used, the FISH to *lacZ* sequences showed a diffuse distribution, which colocalized with the GFP chimeric signal (Figure 2B). When the GFP-MS2 chimera was expressed in cells without any reporter mRNA present (Figure 2C) or with MS2-binding sites deleted from the reporter mRNA (Figure 2D), the GFP fluorescence was mainly nuclear. To determine whether the GFP chimera artifactually induced the particle in the presence of another plasmid, we deleted the *ASH1* reporter of its MS2-binding sites. After galactose induction and FISH for *lacZ* sequences, the RNA could still be seen concentrated in a particle in many cells, although the GFP-MS2 was not (Figure 2D).

In contrast to the single particles we observed with the *ASH1* reporter, endogenous *ASH1* mRNA localized in a number of spots, forming a crescent at the bud tip as detected by FISH (Long et al., 1997; Takizawa et al., 1997). We speculated that this was because the *ASH1* reporter was expressed throughout the cell cycle, while endogeneous *ASH1* mRNA was expressed only transiently during anaphase (Jansen et al., 1996). This hypothesis was tested by galactose induction of the *ASH1* reporter for a short time. Galactose induction within 30 min produced an increase in the cytoplasmic particulate signal (above that in raffinose) that was seen as many small and dim particles localized in the bud. The endogenous *ASH1* gene produced a similar signal, but only in cells at anaphase (Figure 2E). Fusion of two particles to form a larger one could be occasionally observed. This suggested that formation of the single, bright particles in the presence of the *ASH1* mRNA reporter resulted from the continuous high-level expression of the reporter mRNA. To assess whether the particles produced by the *ASH1* reporter could be coassembled with endogeneous *ASH1* mRNA, we induced expression of the reporter for a short time and performed FISH with probes specific for the *ASH1* coding sequence. Indeed, the particle colocalized with some of the endogenous *ASH1* mRNA (Figure 2F). This showed that the *ASH1* reporter could form multimolecular complexes with the endogeneous *ASH1* mRNA.

In the control cells, without the reporters for instance, occasional dim GFP particulate signal could be seen that were not scored as particles because they were dim and because they were never localized in the bud. We measured the fluorescent intensity of this particulate signal and compared it to the bright particles. It was measured to be approximately an order of magnitude dimmer than the particles formed in the presence of the *ASH1* 3′UTR. This particulate signal may represent some aggregation of GFP-MS2 chimera even though we used a mutant version of MS2 reported to be deficient in self-assembly (Lim and Peabody, 1994).

These results indicated that the *ASH1* 3′UTR facilitated the formation of a multi-molecular RNA particle.

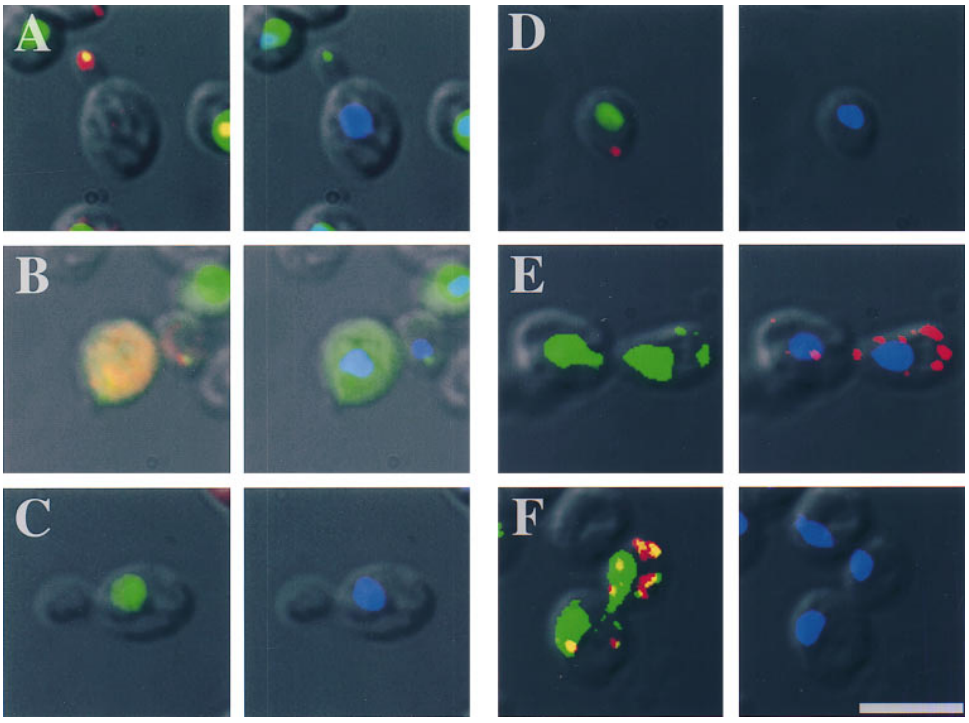

Figure 2. The Bright Particle and Its Localization Are *ASH1* 3′UTR-Dependent

(A) Particle formation and localization of the GFP-MS2 fusion protein (green) in cells (K699) that express the *ASH1* reporter (*lacZ*-MS2-*ASH1* 3′UTR). Probes to *lacZ* used for FISH (red) colocalized (yellow) with the particle. 68% of the cells with GFP signal had a bright, single particle, and 78% of the cells with signal had localized particles. The DAPI signal is to the right of each panel. All samples were fixed.

(B) Diffuse signal from the GFP-MS2 fusion protein in cells (K699) that express the *ADHII* reporter (*lacZ* -MS2-*ADHII* 3′UTR). Probes to *lacZ* used for FISH (red) colocalized (yellow) with the diffuse GFP signal (green). 4% of the cells with GFP signal had a single, bright particle of equivalent intensity to those found in cells containing the *ASH1* reporter and 2% of cells with signal had localized particles.

(C) The GFP-MS2 fusion expressed without the chimeric RNA reporter. 0% of the cells had a bright, single particle and 0% were localized.

(D) The GFP-MS2 expressed with a reporter that does not contain the MS2-binding sites (*lacZ-ASH1* 3′UTR). FISH shows the localization of the *lacZ* containing RNA. 8% of the cells with GFP signal had a single, bright particle equivalent in intensity to those containing the *ASH1* reporter RNA and 0% of these were localized, even though the reporter without the MS2-binding sites still localized.

(E) Cell expressing the *ASH1* reporter (left) simultaneously used for FISH for the endogenous *ASH1* mRNA (red, right). Images were deconvolved to increase the sensitivity of detection and six adjacent planes of the restored image volume superimposed. GFP signal, not resolvable in unrestored images (e.g., A-D and other figures), was detectable using this approach.

(F) A cell prepared as in E, except the endogenous *ASH1* mRNA signal (red) and *ASH1* reporter signal (green) are colocalized (yellow). The transcription sites of the endogenous *ASH1* RNA in the nucleus can be seen (yellow). Bar, 5 μm.

Since these particles could be seen in the mother, and occasionally moving from the mother to the daughter cell, they were likely the vehicle by which *ASH1* mRNA localized. Therefore, it served as an effective marker for mRNA-specific transport and localization.

She2, She3, and *ASH1* mRNA Sequences Are Required To Assemble Particles

The *she* mutants are known to disrupt *ASH1* RNA localization (Long et al., 1997; Takizawa et al., 1997). Therefore, we predicted that the particle should likewise be delocalized in these mutants. In the *she* mutant strains, the most obvious result was that the number of particles was significantly decreased compared to the wild-type (Figure 3A). Those particles that did form did not localize (Figures 3B–3F). In a *she 5* mutant strain, the particle stayed at the bud neck (Figure 3B), also identical to that that has been seen for *ASH1* mRNA using FISH (Long et al., 1997; Takizawa et al., 1997). In a *she3* mutant strain, the single, bright particles dispersed into many smaller particles, none of which localized (Figure 3C). In a *she1/myo4* mutant strain, particles that formed stayed in the mother (Figure 3D). In a *she2* mutant strain, particles were almost completely obliterated. In a *she4* mutant strain, fewer particles were seen and they were not localized (Figure 3F) about half the time, somewhat less than wild-type. This result varied from observations that *ASH1* mRNA delocalizes in this mutant. We used FISH to probe for the *ASH1* reporter mRNA in these cells to verify that it was delocalized. The majority of the reporter mRNA was not localized, but some could be seen in the bud. This observation suggests that RNA that has aggregated into a GFP particle may be capable of localizing. Because the detection of RNA with FISH is more sensitive than with GFP, the nonlocalized RNA can be detected by the probes but not by the GFP. These results suggest that She4p may increase the efficiency of particle formation.

The dependence of the particle formation on the *SHE* genes suggested that some of their proteins may play

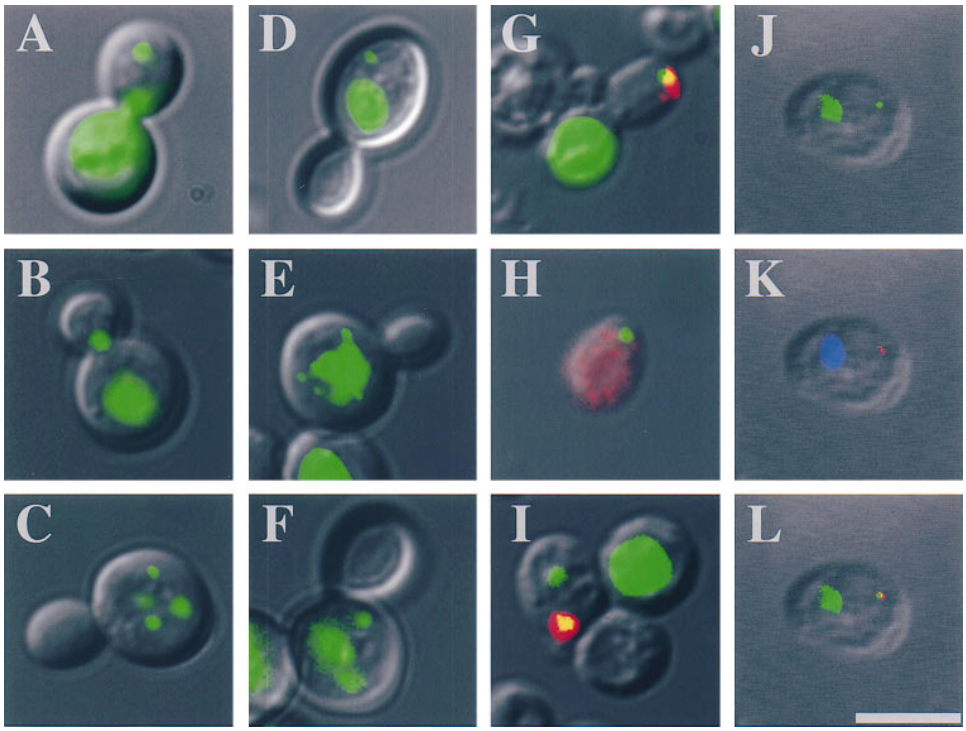

Figure 3. The Effect of the *she* Mutants on Particle Localization and Formation

Yeast strains disrupted for each one of the five *SHE* genes were transformed with the *ASH1* reporter RNA and the GFP-MS2 fusion protein and the resultant particles observed by epifluorescence after fixation. Bar, 5 μm. (A) Wild-type cells (K699). Localization of the particle and its formation is inhibited in (B) *she5* deletion strain (K5205): 36% of cells with signal formed bright, single particles; approximately half of the particles were localized at the bud neck and 2% were localized in the bud. (C) *she3* deletion strain (K5235): 6% formed bright, single particles and 0% were localized in the bud. (D) *she1* deletion strain (K5209): 16% of cells with signal formed bright, single particles and 0% were localized in the bud. (E) *she2* deletion strain (K5547): 0% formed bright, single particles and 0% were localized in the bud. (F) *she4* deletion strain (K5560): 32% formed bright, single particles and 16% with signal were localized in the bud. Colocalization (yellow) of a functional myc-tagged she protein (red) with the particle (green). (G) She1myc. (H) She2myc. (I) She3myc. (J–I) She1myc with nonlocalized particle in nonbudding cell. (Half of the particles showed colocalization with She1myc.)

a structural role. To demonstrate positively whether any of the She proteins are involved structurally in the particle, we introduced a myc tag into the relevant She proteins and reintroduced these constructs into a wild-type reporter strain. Prior to this, the myc-tagged *SHE* proteins were verified to be functional by rescue of the RNA localization phenotype in their respective deletion strains. In a *she1* point mutant strain, the localization of the particle was rescued by She1myc. In cells expressing this She1myc, the signal for the myc colocalized with the localized particle at the bud tip (Figure 3G).

In cells expressing She2myc, the myc immunofluorescence and the particle did not colocalize, despite its requirement for particle rescue (Figure 3H). In contrast to She2myc, the immunofluorescence for She3myc was congruent with the particle, indicating that the particle was associated with this protein, possibly as a structural component (Figure 3I). In support of this, overexpression of She3myc in the *ASH1* reporter strain resulted in abnormally large, ragged granules rather than discrete particles, indicating that She3p is responsible for formation of this aggregation (data not shown). This combined with the fact that particles do not form in a *she3* mutant strain suggests that the particle may require She3p and the specific RNA structural components.

However, since it is known that She1p/Myo4p can localize at the bud tip independent of the RNA (Jansen et al., 1996), colocalization there does not prove a direct association. To determine whether She1/Myo4 was directly associated with the particle, we detected the She1myc and particle simultaneously not at the bud but within the nonbudding cell (3J-L). High-resolution imaging was able to resolve She1myc associated with particles most of the time (in nonbudding cells). This suggests that She1/Myo4 can act to move the particle directly rather than only anchor it at the bud. Direct analysis of the particle movement confirmed this interpretation (see below).

Particle Movement Requires She1/Myo4 and Is Consistent with a Myosin V Motor

Since the particles were bright enough to be followed in living cells, we observed their movement in real time using video microscopy to ascertain if the myosin directly transported the particle from mother to daughter cells. Initially, we observed living cells containing a particle to identify which particles were capable of movement. When a moving particle was identified, it was analyzed for up to 4 min. In the wild-type cells, some

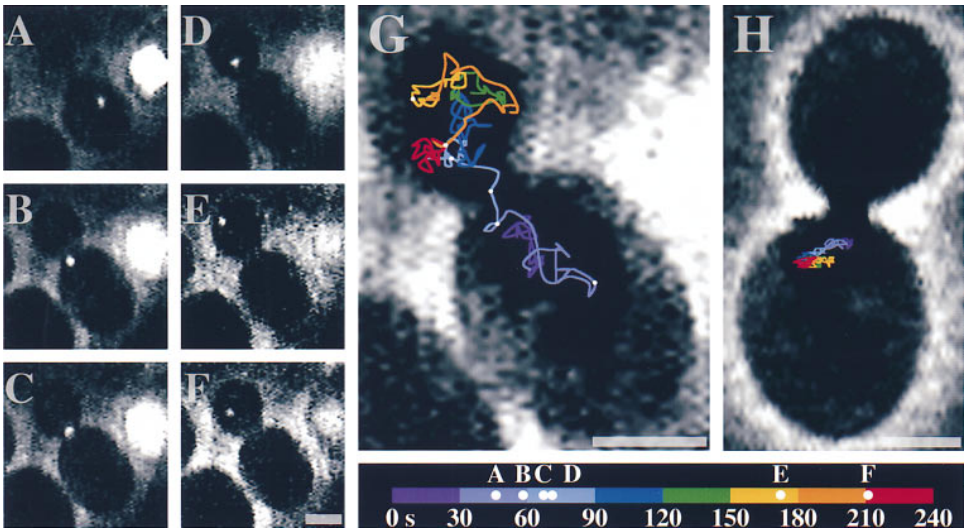

Figure 4. Analysis of Particle Movement

(A–G) Wild-type yeast strain (K699) expressing both the *ASH1* reporter and the GFP-MS2 protein were observed with epifluorescence and bright field microscopy. A cell with minimal nuclear signal was chosen so as not to obscure the particle. Movement of the particle was recorded with a video camera linked to a VCR. Images are presented at indicated intervals. (A–F) Movement of the particle from the mother (nucleated) to the bud (not nucleated). The mRNA particle was analyzed over a period of 4 min, during which it moved a net linear distance of 4.4 μm in a time of 128 sec, over a total pathlength of 23 μm.

A, 46s; B, 58s; C, 67s; D, 71s; E, 172s; and F, 211s. (G) A schematic diagram recapitulates the particle movement over its total path (43 μm per 240 sec). During the period of observation the 30 sec intervals are represented beginning with the coolest colors (purple) and proceeding to the hottest colors (red). The times representing A-F are indicated as white dots on the travel line. The particle spends 180 out of 240 sec in the bud and about 60 sec localized at or near the bud tip. (H) Strain K5209 containing a deletion of *she1* analyzed by the same approach showed significantly less net displacement and stayed within the mother cell, never localizing to the bud tip. Bar, 2 μm. A quick-time movie is available at http://www.molecule.org/supplemental/2/4/437.

movement was observed in about half the cells. Although most of the particles were localized at or near the bud tip, they could occasionally be seen to move from the mother to the bud. This movement could occur bidirectionally, with the particle moving back toward (but not into) the mother and then back to the bud tip. In the mother, sometimes the particle moved around randomly and then "took off" through the bud neck, where velocity was the highest (net displacement per unit of time). Once in the bud, the particle moved in the distal region and occasionally stalled at the bud tip for periods exceeding 1 min.

One of the wild-type particles travelling from mother to bud was analyzed in detail (Figures 4A–4G). The movement was generally directional, but the particle wandered over a path five times longer than the shortest possible distance to the bud tip. This travel path is shown in Figure 4G. The particle moved at velocities that varied between 200–440 nm/sec when time averaged over a moving window of 3 sec. This movement was consistent with that expected for a myosin V motor function reported to be 200–400 nm/sec (Cheney et al., 1993). These results demonstrated that this motor functions to move the RNA into the bud. Presumably this occurs along actin cables. The localization time (mother to bud tip) for the particle was 128 sec. Because of the short time required to localize, the movement of the RNA was therefore a rare event in the steady-state population. This rapid time for RNA transport emphasizes the importance of using living cells to investigate the process of localization, since no other current technique is capable of sub-second time resolution (video rate, 33 frames/sec).

To confirm that the particle movement was due to *SHE1/MYO4*, we investigated particle movement in two *she1/myo4* strains known to disrupt mRNA localization (Long et al., 1997; Takizawa et al., 1997). The first one bears an inactivating point mutation (she1-456; Jansen et al., 1996), and the second one is a deletion strain. The particle formed less efficiently in the deletion strain than in wild-type cells (Figure 4D) and formed as efficiently as in the wild-type in the point-mutant strain. The lack of the movement seen in both of these strains compared to the the wild-type strain was evident; the particle was generally immobile and did not end up in the bud (Figure 4H). Few particles ($<$10%) were observed to exhibit any movement at all. In the few instances when particles moved in the *she1/myo4* deletion strain, they showed no persistence: they did not travel a net distance larger than 0.5 μm, one-tenth of the net distance travelled by the particle in a wild-type strain during the same time period. These results strongly suggest that She1p/Myo4p actively transports *ASH1* reporter particles into the bud.

Discussion

The visualization of RNA movement in a living cell presented a dynamic view of the localization mechanism. Several insights into the localization process resulted from this approach. The first was that this transport occurred via a macromolecular complex, a particle,

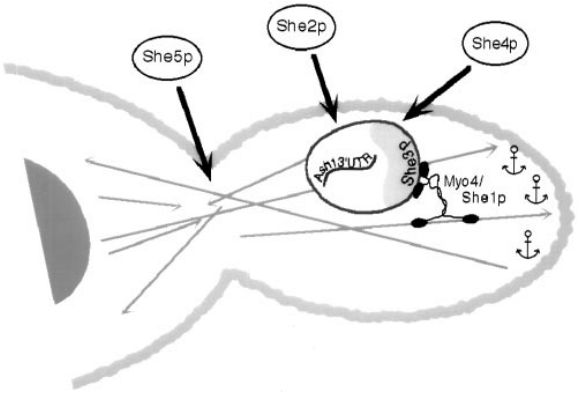

Figure 5. Model of the Particle Movement

The schematic depicts the particle moving directly on actin filaments via She1p in budding yeast. Because She3p was visualized as part of the particle, it is represented along with other, as yet unknown, components. She2p and She4p act on the formation of the particle, illustrated by the arrows. She5p traps the particle at the bud neck. Actin filaments are represented with the barbed end as the arrowhead. The mixed polarity is interpreted from the bidirectional movement of the particle. Once in the bud, the particle stays there, so that the actin filaments with opposite polarity are represented as discontinuous at the neck. Anchors represent potential points of attachment of the particle.

which depends on its existence and localization on a segment of the *ASH1* 3′UTR as did the *lacZ* reporter RNA. The second was that the RNA-dependent particle movement was consistent with the speed generated by a motor, which transported it to its location within a few minutes. Genes required for localization appear to interact with the RNA via this particle.

A specific myosin motor (Haarer et al., 1994) moved this *ASH1* mRNA reporter with the velocity and direction expected of an actin-based motor (Cheney et al., 1993). Confirming this, *she1/myo4* strains were unable to move the reporter into the bud. This suggested that She1p/Myo4p was acting as a motor directly for the transport of the *ASH1* reporter rather than indirectly moving another component to the bud tip that subsequently anchored the mRNA. Further confirming this assumption, we observed the myosin directly associated with the particle. It is reasonable that this mechanism is a direct rather than indirect one, because there are five myosins in yeast (Mermall et al., 1998) and only She1/Myo4 affects the mRNA, even when the other myosins are fully functional. If myosin localized the mRNA by cytoplasmic flow or by moving the actin filaments on which the RNA is bound, it would be difficult to conceive of a mechanism that would be selective for the particle movement without direct interaction (see model in Figure 5).

By analyzing the motion of the particle, the polarity of the actin filaments on which the myosin is moving could be deduced to be with the barbed end toward the bud tip. Despite considerable physiological information on the yeast cytoskeleton, structural knowledge, for instance of the polarity of the actin cables, is very limited (Adams and Pringle, 1984; Kilmartin and Adams, 1994; Li et al., 1995; Ayscough and Drubin, 1996; Doyle and Botstein, 1996; Ayscough et al., 1997; Nasmyth and Jansen, 1997; Vaduva et al., 1997). The observed retrograde motion could be a result of the myosin detaching from the actin, or movement along filaments of reverse polarity or association with some as yet undetermined structure.

It is interesting to note that the *ASH1* reporter moved to the bud but did not seem to anchor there; it continued to move around. This suggested that the sequences in the *ASH1* 3′UTR, while sufficient to direct the reporter to the bud (transport), may not contain the information sufficient to keep it at the cortex (anchoring). Such information appears to be contained within the coding region, as reporter RNAs fused to sequences in the open-reading frame show a tight crescent at the bud tip (data not shown). This suggests that localization involves at least two steps, transport and anchoring, as has been predicted in previous work (Yisraeli et al., 1990; Sundell and Singer, 1991).

Importantly, actomyosin is only one of the means by which mRNA can move. A number of systems appear to localize mRNAs through microtubules including *Drosophila* oocytes and embryos (St. Johnston, 1995), *Xenopus* oocytes (Yisraeli et al., 1990), and neurons (Bassell et al., 1994, 1998). Recent evidence suggested kinesin as a motor for myelin basic protein mRNA in oligodendrocytes (Carson et al., 1997). While these systems seem divergent in their mechanisms, isolation of proteins binding localization sequences in β-actin mRNA in fibroblasts (zipcode binding protein 1; Ross et al., 1997), which uses an actomyosin system, and the sequences in Vg1 mRNA, which uses microtubules, reveals an identity in these RNA-binding proteins (Deshler et al., 1998; Havin et al., 1998). Possibly either identical proteins can convert to different motors or the particle contains bifunctional motors. For instance, myosin and dynein are known to interact (Benashski et al., 1997) and particles can travel on multiple cytoskeletal elements (Rodionov et al., 1998).

The transport of the reporter could be visualized because of the formation of a particle. Because the particle formation was dependent on specific sequences in the *ASH1* 3′ UTR sufficient for directing a *LacZ* reporter RNA to the bud and because it could not localize in *she* mutant strains, the particle served as a reporter for localization. She proteins and sequences from the *ASH1* mRNA 3′ UTR participate in forming this particle. The particle may be directly associated with the myosin, possibly through She3p. This is supported by evidence that She3p and She1p/Myo4p colocalize with the particle. Both She3p and She1p also localize to the bud tip during anaphase (Jansen et al., 1996) but then become delocalized, presumably leaving the mRNA in place at the tip. In She5p/Bni1p, the particle becomes arrested at the bud neck, as does the *ASH1* mRNA (Long et al., 1997). This protein is a member of the formin family of proteins and has been shown to be important in polarizing the actin cytoskeleton and is itself localized to the bud tip (Evangelista et al., 1997). Other She proteins most likely interact with the particle during its formation but do not form part of its structure. She2p is required for particle formation. She4p appears to facilitate particle assembly but is not essential. It is not known whether She4p is a structural component. *SHE4* is also required for receptor internalization, which is decreased but not

abolished in a *she4* deletion strain, indicating that this gene has a partial penetrance phenotype (Wendland et al., 1996). Within the particle, the RNA could form a structural framework, analogous to how the ribosome forms around the ribosomal RNA. The proteins associating with the RNA and with the She proteins remain to be elucidated.

The particle described here may have some similarity to the particles observed in other systems. In the localization of *bicoid* mRNA in *Drosophila* (Ferrandon et al., 1997), the 3′ UTR of the mRNA induces the formation of a particle containing Staufen protein, by forming a multimolecular complex through RNA–RNA interactions. Staufen protein is a helicase required for the anchoring of the RNA late in localization at the anterior pole of the oocyte, presumably on the spindle microtubules (Ferrandon et al., 1994). In vertebrate systems that localize mRNAs, whether by actin filaments (Sundell and Singer, 1991) or by microtubules (Bassell et al., 1998), granules appear to be a universal feature for transporting and/or anchoring these mRNAs (Ainger et al., 1993; Knowles et al., 1996; Glotzer et al., 1997). This suggests that the particle mechanism of localization may be phylogenetically conserved from yeast. However, our data do not exclude that the endogeneous mRNA could be transported as single molecules. Early in the induction of the *ASH1* reporter by galactose, many small particles can be seen, some of which are localized. Eventually, overexpression of the reporter results in the large particle, presumably formed from coalescence of the smaller particles. We are as yet unable to determine whether single molecules of *ASH1* mRNA can be transported as a "mini-particle" since we cannot yet visualize single RNA molecules using GFP.

The interaction of the RNA with the proteins required for localization may make a structural entity specialized for this function, which we term the *locasome*. It is reminiscent of similar RNA–protein complexes specialized for a particular function, such as the ribosome, or the spliceosome, both of which contain RNA as part of their structural basis.

The methods described here for visualizing RNA movement in living cells could also be applied to the investigation of any RNA–protein complex, such as those involved in RNA processing, nuclear export, or intranuclear targeting. Additionally, it is not restricted to yeast; the approach is applicable to higher eucaryotic cells as well (data not shown). Finally, the GFP chimera coupled with the *ASH1* reporter will provide a rapid and convenient way to screen mutants affecting RNA localization.

Experimental Procedures

Yeast Genotypes

Wild type, k699 genotype (Mata, *his3-11,leu2-3,ade2-1, trp1-1*, *ura3*, *ho*; *can1-100*); *she1*, K5209 genotype (Mata, *his3,leu2,ade2*, *trp1*, *ura3*, *can1-100*, *she1::URA3*); *she2*, K5547 genotype (Matα, *his3, leu2,ade2*, *trp1*, *ura3*, *HO-ADE2*, *HO-CAN1*, *she2::URA3*); *she3*, K5235 genotype (Matα, *his3,leu2,ade2*, *trp1*, *ura3,can1-100*, *she3::URA3*); *she4*, K5560 genotype (Matα, *his3,leu2,ade2*, *trp1*, *ura3*, *she4::URA3*); and *she5*, K5205 genotype (Matα, *his3,leu2,ade2, trp1*, *ura3*, *can1-100*, *she5::URA3*).

The Reporter Genes Containing the MS2-Binding Sites

Two repeats of a high-affinity MS2-binding site were amplified by PCR from the pIIIA-MS2–2 plasmid (gift of M. Wickens; SenGupta et al., 1996) with the following oligonucleotides: 5′ CTAGCTGGATC CTAAGGTACCTAATTGCCTAGAAAACATGAGGA, and 5′ ATGCTA AGATCTAATGAACCCGGGAATACTGCAGACATGGGAGAT. The PCR product was digested with BamHI and BglII and self-ligated in presence of the same enzyme to multimerize the MS2 sites in a head to tail fashion. The DNA corresponding to a six-repeat of the MS2 site was gel purified and ligated into the BamHI and BglII sites of pSL1180 (Pharmacia), to give the plasmid pSL-MS2–6. The plasmids pXR55 (*ASH1* 3′UTR) and pXR2 (*ADHII* 3′UTR) were generated, respectively, by subcloning the *lacZ-ASH1* 3′UTR and the *lacZ-ADH II* reporter constructs into the yeast vector YEplac195 (Gietz and Sugino, 1988) as a PstI/EcoRI restriction fragment generated by PCR and DNA restriction digests. The *lacZ-ASH1* 3′UTR cassette originated from plasmid pXMRS25, and the *lacZ-ADHII* cassette originated from plasmid pHZ18-polyA (Long et al., 1995, 1997). Both pXR55 and pXR2 contain the *URA3* selectable marker, the 2 μ origin of replication, and express the reporter mRNAs from a galactose-inducible promoter. pSL-MS2-6 was digested by MscI and EcoRV and cloned at the KpnI site of pXR55, to give pGal-*lacZ*-MS2-*ASH1/URA*, or digested by BamHI and NheI and cloned between the BglII and XbaI sites and pGal-*lacZ-ADHII/URA*, to give pGal-*lacZ*-MS2-*ADHII/URA*. The *GAL-lacZ*-MS2-*ASH1* reporter cassette was then moved into YEplac 112, *TRP1* selectable, 2 μ plasmid (Ibid.) by cloning the ScaI-EcoRI fragment of p*GAL-lacZ*-MS2-*ASH1/URA* into the ScaI and EcoRI sites of pYEplac112, to give p*GAL-lacZ*-MS2-*ASH1/TRP*.

The GFP-MS2 Expression Vector

A yeast optimized version of the GFP cDNA (Cormack et al., 1997) was amplified by PCR with the following oligonucleotides: 5′ GTATC AGCGGCCGCTTCTAAAGGTGAAGAATTA (yGFP/5′) and 5′ TGACC TGTCGACTTTGTACAATTCATCCAT (yGFP/3′). The resulting PCR product was then digested with NotI. A plasmid containing the HA-tagged MS2 mutant protein dlFG was obtained from Philippe Couttet (IJM, Paris), and the cDNA was PCR amplified with the following oligonucleotides: 5′ TCAGTCGCGGCCGCGTAGATGCCGGAGTTT (MS2/3′) and 5′ TAGCATGGATCCACC*ATGCCAAAAAAGAAAAGAA AAAGTT*GGCTACCCCTACGACGTGCCCGA (NLS-MS2/5′). The initiator ATG followed by the SV40 nuclear localization sequence is depicted in italic letters. The resulting PCR product was then digested with NotI. The two PCR products were then ligated together, and the GFP-MS2 chimeric cDNA was reamplified with the GFP/3′ and the NLS-MS2/5′ oligonucleotides. The resulting PCR product was then digested with BamHI and SalI and ligated into the corresponding site of the *LEU2* selectable, 2 μ pG14 plasmid (Lesser and Guthrie, 1993; a gift of J. Warner) to give *pGFP-MS2/LEU*.

Expressing the Reporters and the GFP-MS2

The strain K699 (Mata, *trp1-1*, *leu2-3*, *his3-11,ura3*, *ade2-1*, *ho*, *can1-100*) was transformed with various combinations of the episomal vectors described above and below and selected on the appropriate selection media to maintain the plasmids. Yeast cells were then grown to mid-log phase in sythetic media containing 2% raffinose. Cells were subsequently induced with 3% galactose for 3 hr or the indicated times, to induce expression of the reporter mRNA. Due to the variable expression levels of the two plasmids, some cells have particles without much GFP nuclear signal, and some cells have strong GFP signal without visible particles.

Measurement of Particle Brightness

Particles comprised of a range of intensities, the single, bright particles in cells with the *ASH1* reporter and the much weaker particles in the control cells (e.g., Figures 2B–2D), were measured by capturing digital images and circling the particles using Cellscan software (Scanalytics, VA) and the total fluorescent intensity was obtained. The single, bright particle had a fluorescent intensity 10.7 times brighter than the weaker particles commonly found in the controls (Figures 2B–2D) and thus were easy to score. Particle counts were scored by three individuals. In different isolates of the wild-type strain, fixed cells containing the bright, single particles ranged from

54%–68% (e.g., Figures 2A and 4A); localization in these cells ranged from 64%–78%.

In Situ Hybridization and Immunofluorescence

Yeast cells were processed for in situ hybridization as previously described (Long et al., 1995, 1997), except that the hybridization mixture and the wash solutions contained only 10% formamide. The oligo-Cy3-conjugated probes were also previously described (Long et al., 1995, 1997). Cells were prepared for immunofluorescence as for in situ hybridization. After permeabilization overnight in 70% ethanol, the cells were rehydrated in antibody buffer (2X SSC, 8% formamide) for 10 min at room temperature and were then incubated in antibody buffer containing 0.2% RNAse DNAse free BSA and an anti-myc antibody (gift from K. Nasmyth) diluted 1:5, for 1 hr at 37°C. Cells were then washed for 30 min at room temperature in antibody buffer and were further incubated for 1 hr at 37°C with a Cy3-conjugated anti-mouse secondary antibody diluted 1:700, in antibody buffer. Cells were then mounted in mounting media (Long et al., 1995, 1997) after a final 30 min wash at room temperature in antibody buffer.

Image Acquisition and Processing

Images were captured using CellSCAN software (Scanalytics, Fairfax, VA) on an Optiplex GXpro computer (Dell, Austin, TX) with a CH-250 16-bit, cooled CCD camera (Photometrics, Tuscon, AZ) mounted on a Provis AX70 fluorescence microscope (Olympus, Melville, NY) with a PlanApo 60x, 1.4 NA objective (Olympus) and HiQ bandpass filters (Chroma Technology, Brattleboro, VT). The fluorescence illumination was controlled by the software using a Uniblitz VS25 shutter (Vincent Associates, Rochester, NY). When images were restored (Figures 2E and 2F), a three-dimensional data set, composed of 20–25 images separated by 200 nm in the axial direction, was acquired and deconvolved with an acquired point spread function (PSF) using EPR software (Scanalytics). The software controlled the axial position of the objective using a PZ54 E piezoelectric translator (Physik Instrumente, Costa Mesa, CA). The PSF is a data set, composed of 40–50 images separated by 200 nm in the axial direction, of a fluorescent microsphere (Molecular Probes, Eugene, OR) that was 200 nm in diameter. A single median plane was recorded for blue filtered images.

Colocalization Analysis of the GFP Particle and She1p/Myo4pmyc

Twenty cells were analyzed for colocalization of the particle and She1myc. Thirty optical sections of each cell were taken and the red and green images superimposed for each image plane. The number of particles colocalizing with She1myc in the same plane were counted. About half (45%) were colocalized with She1myc. For a control, wild-type cells containing GFP particles but without She1myc were evaluated by identical methods. No colocalization was observed with the immunofluorescent antibodies.

Cloning and Epitope Tagging of the *SHE* Genes

The *SHE* genes were isolated from yeast genomic DNA (strain K699) by PCR. Primers were designed to obtain a PCR fragment of the respective *SHE* gene to include 1 kb of the promoter as well as 1 Kb of the 3′-UTR region. The cloned *SHE* genes were subcloned into YEplac112 and YCplac22 and transformed into yeast strains disrupted for the respective gene and tested for functionality by rescue of *ASH1* mRNA localization as determined using FISH.

A unique restriction site was introduced after the corresponding start codon or in front of the respective stop codon for each of the *SHE* genes (except *SHE1*) using a splicing through overlap extension strategy. Basically, four primers were designed per SHE gene, which gave rise to two PCR fragments that had an overlapping sequence containing a single restriction site at the N- or C-terminal part of the gene. These fragments served as template in a second PCR step to amplify the final fragment, which was cloned in YEplac112.

Three Myc epitopes were introduced in these unique sites using BamHI (in the case of *SHE3*) or XbaI (*SHE2*) fragments of a Myc epitope cassette (from plasmid pC3003, gift from K. Nasmyth). In the case of *SHE1/MYO4*, a C-terminal SpeI site (25 aa upstream of the stop codon) was used to subclone a SpeI fragment of a c-Myc epitope cassette (from plasmid pC3390, gift from K. Nasmyth) containing nine Myc epitopes. Expression of the Myc-epitope-tagged proteins was also shown by Western blots.

After demonstrating functionality, *SHE-myc* plasmids were transformed into K699, containing a wild-type locus for each *SHE* gene with the GFP-reporter plasmids for colocalization studies.

Methods for the Video Analysis

Live cells were mounted between two coverslips and visualized on an inverted microscope (Nikon, Melville, NY) with a PlanApo 60×, 1.4 NA, Ph4 objective (Nikon) using simultaneous brightfield and epifluorescence illumination. Live video was captured using a C2400 Silicon Intensified Tube Camera (Hamamatsu, Oakbrook, IL) with a 2× eyepiece and recorded on video tape in S-VHS format. Appropriate sequences from the tape were digitized at a rate of one frame per second using NIH Image software (NIH, Bethesda, MD) with a frame size of 640 × 480 pixels on a Power Macintosh 7600 computer (Apple, Cupertino, CA) with S-Video interface. Using NIH Image, the particle's position in each captured frame was tabulated and then used to calculate distance travelled and speed.

Motor Analysis

Four min of video analysis of a specific particle moving from mother to bud was analyzed at 1 sec intervals. The movement was then averaged over a moving time window of 3-sec time points and spatially filtered to require a total net travel of five pixels (about 0.5 μm) during this time window. The wild-type movement throughout the time frame resulted in 15 of these 3 sec "jumps" at intervals ranging from 5 to 30 sec. Distances moved during the time frame were from 0.6 to 1.4 μm. Average speeds per jump ranged from 200–440 nm/sec. The *she1* deletion strain showed no movement when subjected to this spatial filtering. Effectively, this approach subtracts the background *she1* movement from the wild-type to reveal the motility characteristics of the She1/Myo4p.

Acknowledgments

Supported by GM 54887 and GM 57071 to R.H.S., Canadian Fonds pour la Formation de Chercheurs et l'Aide à la Recherche fellowship to P.C., and F32-HD08088 to R.M.L. The authors thank Michael Rosbash and John Warner for helpful discussions.

Received May 14, 1998; revised August 10, 1998.

References

Adams, A.E.M., and Pringle, J.R. (1984). Relationships of actin and tubulin distribution of wild type and morphogenetic mutant *Saccharomyces cerevisiae*. J. Cell Biol. *98*, 934–945.

Ainger, K., Avossa, D., Morgan, F., Hill, S.J., Barry, C., Barbarese, E., and Carson, J.H. (1993). Transport and localization of exogenous myelin basic protein mRNA microinjected into oligodendrocytes. J. Cell Biol. *123*, 431–441.

Amon, A. (1996). Mother and daughter are doing fine: asymmetric cell division in yeast. Cell *84*, 651–654.

Ayscough, K.R., and Drubin, D.G. (1996). Actin: general principles from studies in yeast. Annu. Rev. Cell Dev. Biol. *12*, 129–160.

Ayscough, K.R., Stryker, J., Pokala, N., Sanders, M., Crews, P., and Drubin, D.G. (1997). High rates of actin filament turnover in budding yeast and roles for actin in establishment and maintenance of cell polarity revealed using the actin inhibitor latrunculin-A. J. Cell Biol. *137*, 399–416.

Bassell, G.J., Singer, R.H., and Kosik, K.S. (1994). Association of poly(A) mRNA with microtubules in cultured neurons. Neuron *12*, 571–582.

Bassell, G., Zhang, H., Byrd, A., Femino, A., Singer, R., Taneja, K., Lifshitz, L., Herman, I., and Kosik, K. (1998). Sorting of beta-actin mRNA and protein to neurites and growth cones in culture. J. Neurosci. *18*, 251–265.

Benashski, S.E., Harrison, A., Patel-King, R.S., and King, S.M. (1997).

Dimerization of the highly conserved light chain shared by dynein and myosin V. J. Biol. Chem. *272*, 20929–20935.

Bobola, N., Jansen, R.-P., Shin, T.H., and Nasmyth, K. (1996). Asymmetric accumulation of Ash1p in postanaphase nuclei depends on a myosin and restricts yeast mating-type switching to mother cells. Cell *84*, 699–709.

Carson, J.H., Worboys, K., Ainger, K., and Barbarese, E. (1997). Translocation of myelin basic protein mRNA in oligodendrocytes requires microtubules and kinesin. Cell Motil. Cytoskeleton *38*, 318–328.

Cheney, R.E., O'Shea, M.K., Heuser, J.E., Coelho, M.V., Wolenski, J.S., Espreafico, E.M., Forscher, P., Larson, R.E., and Mooseker, M.S. (1993). Brain myosin-V is a two-headed unconventional myosin with motor activity. Cell *75*, 13–23.

Cormack, B., Bertram, G., Egerton, M., Gow, N., Falkow, S., and Brown, A. (1997). Yeast-enhanced green fluorescent protein (yEGFP) a reporter of gene expression in *Candida albicans*. Microbiology *143*, 303–311.

Deshler, J.O., Highett, M.I., Abramson, T., and Schnapp, B.J. (1998). A highly conserved RNA-binding protein for cytoplasmic mRNA localization in vertebrates. Curr. Biol. *1*, 489–496.

Doyle, T., and Botstein, D. (1996). Movement of yeast cortical actin cytoskeleton visualized in vivo. Proc. Natl. Acad. Sci. USA *93*, 3886–3891.

Evangelista, M., Blundell, K., Longtine, M.S., Chow, C.J., Adames, N., Pringle, J.R., Peter, M., and Boone, C. (1997). Bni1p, a yeast formin linking cdc42p and the actin cytoskeleton during polarized morphogenesis. Science *276*, 118–122.

Ferrandon, D., Elphick, L., Nusslein-Volhard, C., and St. Johnston, D. (1994). Staufen protein associates with the 3′UTR of *bicoid* mRNA to form particles that move in a microtubule-dependent manner. Cell *79*, 1221–1232.

Ferrandon, D., Koch, I., Westhof, E., and Nusslein-Volhard, C. (1997). RNA-RNA interaction is required for the formation of specific bicoid mRNA 3′ UTR-staufen ribonucleoprotein particles. EMBO J. *16*, 1751–1758.

Fouts, D., True, H., and Celander, D. (1997). Functional recognition of fragmented operator sites by R17/MS2 coat protein, a translational repressor. Nucleic Acids Res. *25*, 4464–4473.

Gietz, R., and Sugino, A. (1988). New yeast-*Escherichia coli* shuttle vectors constructed with in vitro mutagenized yeast genes lacking six-base pair restriction sites. Gene *74*, 527–534.

Glotzer, J.B., and Ephrussi, A. (1996). mRNA localization and the cytoskeleton. Cell Dev. Biol. *7*, 357–365.

Glotzer, J.B., Saffrich, R., Glotzer, M., and Ephrussi, A. (1997). Cytoplasmic flows localize injected oskar RNA in *Drosophila* oocytes. Curr. Biol. *7*, 326–337.

Haarer, B.K., Petzold, A., Lillie, S.H., and Brown, S.S. (1994). Identification of MYO4, a second class V myosin gene in yeast. J. Cell Sci. *107*, 1055–1064.

Havin, L., Git, A., Elisha, Z., Oberman, F., Yaniv, K., Pressman Schwartz, S., Standart, N., and Yisraeli, J.K. (1998). RNA binding protein conserved in both microtubule and microfilament-based RNA localization. Genes Dev., in press.

Jansen, R.-P., Dowzer, C., Michaelis, C., Galova, M., and Nasmyth, K. (1996). Mother cell-specific *HO* expression in budding yeast depends on the unconventional myosin Myo4p and other cytoplasmic proteins. Cell *84*, 687–697.

Kilmartin, J., and Adams, A.E.M. (1994). Structural rearrangements of tubulin and actin during the cell cycle of the yeast *Saccharomyces cerevisiae*. J. Cell Biol. *98*, 922–933.

Knowles, R.B., Sabry, J.H., Martone, M.A., Ellisman, M., Bassell, G.J., and Kosik, K.S. (1996). Translocation of RNA granules in living neurons. J. Neurosci. *16*, 7812–7820.

Lesser, C.F., and Guthrie, C. (1993). Mutational analysis of pre-mRNA splicing in *Saccharomyces cerevisiae* using a sensitive new reporter gene, CUP1. Genetics *133*, 851–863.

Li, R., Zheng, Y., and Drubin, D.G. (1995). Regulation of cortical actin cytoskeleton assembly during polarized cell growth in budding yeast. J. Cell Biol. *128*, 599–615.

Lim, F., and Peabody, D.S. (1994). Mutations that increase the affinity of a translational repressor for RNA. Nucleic Acids Res. *22*, 3748–3752.

Long, R.M., Elliott, D.J., Stutz, F., Rosbash, M., and Singer, R.H. (1995). Spatial consequences of defective processing of specific yeast mRNAs revealed by fluorescent in situ hybridization. RNA *1*, 1071–1078.

Long, R.M., Singer, R.H., Meng, X., Gonzalez, I., Nasmyth, K., and Jansen, R.-P. (1997). Mating type switching in yeast controlled by asymmetric localization of ASH1 mRNA. Science *277*, 383–387.

Mermall, V., Post, P.L., and Mooseker, M.S. (1998). Unconventional myosins in cell movement, membrane traffic, and signal transduction. Science *279*, 527–533.

Nasmyth, K., and Jansen, R.P. (1997). The cytoskeleton in mRNA localization and cell differentiation. Curr. Opin. Cell Biol. *9*, 396–400.

Rodionov, V.I., Hope, A.J., Svitkina, T.M., and Borisy, G.G. (1998). Functional coordination of microtubule-based and actin-based motility in melanophores. Curr. Biol. *8*, 165–168.

Ross, A., Oleynikov, Y., Kislauskis, E.H., Taneja, K.L., and Singer, R.H. (1997). Characterization of the β-actin zipcode binding protein. Mol. Cell Biol. *17*, 2158–2165.

Schena, M., Picard, D., and Yamamoto, K.R. (1991). Guide to yeast genetics and molecular biology. In Methods in Enzymology, C. Guthrie and G.R. Fink, eds. (New York: Academic Press), pp. 389–398.

SenGupta, D., Zhang, B., Kraemer, B., Pochart, P., Fields, S., and Wickens, M. (1996). A three-hybrid system to detect RNA-protein interactions in vivo. Proc. Natl. Acad. Sci. USA *93*, 8496–8501.

Sil, A., and Herskowitz, I. (1996). Identification of an asymmetrically localized determinant, Ash1p, required for lineage-specific transcription of the yeast HO gene. Cell *84*, 711–722.

Steward, O., and Singer, R.H. (1997). The intracellular RNA sorting system: postal zones, zip codes, mail bags and mail boxes. In mRNA Metabolism and Post-Transcriptional Gene Regulation. (New York: Wiley-Liss, Inc.), pp. 127–146.

St. Johnston, D. (1995). The intracellular localization of messenger RNAs. Cell *81*, 161–170.

Strathern, J.N., and Herskowitz, I. (1979). Asymmetry and directionality in production of new cell types during clonal growth: the switching pattern of homothallic yeast. Cell *17*, 371–381.

Sundell, C.L., and Singer, R.H. (1991). Requirement of microfilaments in sorting actin messenger RNA. Science *253*, 1275–1277.

Takizawa, P., Sil, A., Swedlow, J., Herskowitz, I., and Vale, R. (1997). Actin-dependent localization of an RNA encoding a cell-fate determinant in yeast. Nature *389*, 90–93.

Vaduva, G., Nartin, N.C., and Hopper, A.K. (1997). Actin-binding verprolin is a polarity development protein required for the morphogenesis and function of the yeast actin cytoskeleton. J. Cell Biol. *139*, 1821–1833.

Valegard, K., Murray, J., Stonehouse, N., van den Worm, S., Stockley, P., and Liljas, L. (1997). The three-dimensional structures of two complexes between recombinant MS2 capsids and RNA operator fragments reveal sequence-specific protein-RNA interactions. J. Mol. Biol. *270*, 724–738.

Wendland, B., McCaffery, M., Xiao, Q., and Emr, S. (1996). A novel fluorescence activated cell sorter-based screen for yeast endocytosis mutants identifies a yeast homologue of mammalian eps15. J. Cell Biol. *135*, 1485–1500.

Yisraeli, J.K., Sokol, S., and Melton, D.A. (1990). A two-step model for the localization of maternal mRNA in *Xenopus* oocytes: involvement of microtubules and microfilaments in the translocation and anchoring of Vg-1 mRNA. Development *108*, 289–298.